DOI: 10.3901/CJME.2015.0908.110, available online at www.springerlink.com; www.cjmenet.com

Welding Deviation Detection Algorithm Based on Extremum of Molten Pool Image Contour

ZOU Yong[1, 2, *], JIANG Lipei[2], LI Yunhua[1], XUE Long[2], HUANG Junfen[2], and HUANG Jiqiang[2]

1 *College of Automation Science and Electrical Engineering, Beihang University, Beijing 100191, China*
2 *Optical Electromechanical Equipment Technology Key Laboratory of Beijing, Beijing Institute of Petrochemical Technology, Beijing 102617, China*

Received June 23, 2015; revised August 31, 2015; accepted September 8, 2015

Abstract: The welding deviation detection is the basis of robotic tracking welding, but the on-line real-time measurement of welding deviation is still not well solved by the existing methods. There is plenty of information in the gas metal arc welding(GMAW) molten pool images that is very important for the control of welding seam tracking. The physical meaning for the curvature extremum of molten pool contour is revealed by researching the molten pool images, that is, the deviation information points of welding wire center and the molten tip center are the maxima and the local maxima of the contour curvature, and the horizontal welding deviation is the position difference of these two extremum points. A new method of weld deviation detection is presented, including the process of preprocessing molten pool images, extracting and segmenting the contours, obtaining the contour extremum points, and calculating the welding deviation, etc. Extracting the contours is the premise, segmenting the contour lines is the foundation, and obtaining the contour extremum points is the key. The contour images can be extracted with the method of discrete dyadic wavelet transform, which is divided into two sub contours including welding wire and molten tip separately. The curvature value of each point of the two sub contour lines is calculated based on the approximate curvature formula of multi-points for plane curve, and the two points of the curvature extremum are the characteristics needed for the welding deviation calculation. The results of the tests and analyses show that the maximum error of the obtained on-line welding deviation is 2 pixels(0.16 mm), and the algorithm is stable enough to meet the requirements of the pipeline in real-time control at a speed of less than 500 mm/min. The method can be applied to the on-line automatic welding deviation detection.

Keywords: welding deviation, welding seam tracking, molten pool contour, curvature extremum, gas metal arc welding(GMAW)

1 Introduction

Automation and robotics is the longer-term trend of welding technology. The welding deviation detection is more essential for tracking control which is one of the key technologies for automatic welding. Several methods of welding tracking have been developed based on the deviation detection sensors such as contact type sensor[1], arc sensor[2], capacitance sensor[3], electromagnetic sensor[4], ultrasonic sensor[5], infrared sensor[6], and visual sensor[7], etc. Among them, the seam tracking technology based on vision sensing is a hotspot and has attracted the attentions of more and more researchers[8].

In the progress of manual welding, the welder can judge and well-control the welding operation through observing the molten pool and the welding torch. It means that there are enough signals in the images of molten pool and the welding torch which are needed for welding process control. The automatic detection and the control of welding process based on molten pool have been studied in the recent years with different welding methods such as gas tungsten arc welding(GTAW), gas metal-arc welding(GMAW), plasma arc welding(PAW), laser welding and so on[9–13]. The main researches have been focused on visual detection of weld pool shape, weld pool edge extraction and recognition, weld pool image feature analysis and penetration control, etc[14–21]. GTAW is more stable in the welding process, and is easier to get a clear weld pool image, so it has been one of the earliest and most researched welding methods. GAO, et al[22], analyzed the characteristics of the centroid of GTAW pool images, established a centroid algorithm using least square linear regression method, and computed the deviations between the arc tip and weld seam centerline.

GMAW is an efficient, convenient, and widely used method which can realize automatic welding easily. But it is more difficult to detect and analyze the weld pool images comparing with GTAW because of more interferences[23] such as spatters dusts, strong arc light, smoke and others. BASKORO, et al[24], proposed the monitoring of the molten

* Corresponding author. E-mail: zouyong@bipt.edu.cn
Supported by National Natural Science Foundation of China(Grant Nos. 51275051, 51505035), National Hi-tech Research and Development Program of China(863 Program, Grant No. 2009AA04Z208), and Beijing Education Commission Innovation Ability Upgrade Program of China (Grant No. TJSHG201510017023)

pool images during pipe welding in GMAW, using the machine vision as a sensor. LIU, et al[25], presented a low-cost camera-based sensor system for closed-loop control in GMAW without using external illumination. The 2D shape of the weld pool was able to extract in real time by a carefully selected optical filtering and an active contour-based tracking of the weld pool boundary. FAN, et al[26], established an image sensing system and extracted the edge of GMAW molten pool images clearly by the processing of morphological opening method and Prewitt edge detection operator. YUE, et al[27], proposed an adaptive vision detection method of weld pool, attained vivid weld pool images of GMA pulse welding and GMA short-circuit welding. LI, et al[28], gathered the welding seam image for pipe-line back welding of metal active gas(MAG), and extracted the weld pool edge using the Chan-Vese model. WU, et al[29], detected the weld pool edge of aluminum alloy metal inert gas(MIG) based on the pulse coupled neural network. XUE, et al[30], detected the molten pool edge and weld line for CO_2 welding based on B-spline wavelet. LI, et al[31], designed a pool imaging system for pipe welding, detected the deviation of the pool and groove, and calculated the vibration amplitude and frequency of molten pool.

A few literatures have introduced the detection methods of seam tracking deviation from the GMAW molten pool image. LIU, et al[32], designed a weld pool image sensor and obtained pulse MIG welding pool image in V groove that can be used in seam tracking, but it was not introduced how to use the pool image to get the welding deviation. LI, et al[33], extracted one side seam edge of pipeline MAG, selected the other side edge according to the results of Sobel transform and seam distance, and determined the weld center by the inter-frame mean method. The initial contour position must be approximately and manually given, and the other side seam position may differ a lot from the actual edge. BAE, et al[34], developed a vision sensing system for automatic GMAW root pass welding of steel pipeline, acquired weld pool images in short circuit welding, and got the welding deviation according to the position of groove center and wire center. But the groove center is usually not coincident with the pool center. ZOU, et al[35], proposed a weld pool deviation extraction algorithm of GMAW robot, used the molten pool front tip as the groove center, obtained the welding deviation on the basis of the pixel value between the wire center and molten front tip center . The extraction result of the molten pool front tip affects directly the accuracy of deviation.

The welding deviation usually refers to the most important deviation in the horizontal direction. A welding deviation algorithm based on curvature extremum of molten pool contour is proposed for seam tracking of the pipeline in all-position root welding. Wavelet transform is used to extract the edge contour of molten pool images, the wire center and molten pool tip center are positioned by the curvature extremum algorithm of the molten pool contour. The welding deviation can be obtained more rapidly and accurately, which is essential for the subsequent automatic control of welding robot.

2 System Description

2.1 Composition of the System

The system of welding deviation for pipeline all-position GMAW molten pool is shown as Fig. 1. It composes of a welding robot, a welding power machine, a CCD camera, a industrial computer image acquisition and processing system, and a pipeline, etc. Fig. 1(a) is the practical system and Fig. 1(b) is the schematic diagram.

(a) Practical system

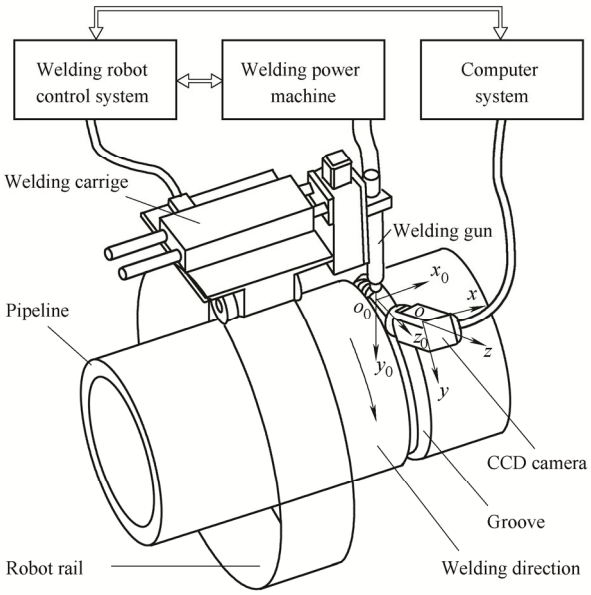

(b) Schematic diagram

Fig. 1. Experimental system of welding deviation

The automatic welding machine is a kind of rail-type and self-made all-position welding robot named as GDC-4[36], which is composed of a circular rail, a welding carriage, a remote control box, the control system and a welding power machine etc. The robot can hold the torch rotating around the pipeline and implement the automatic welding. The robot controller is S7-200 of Siemens PLC and the welding power machine is Pulse MIG-500 of Autai.

The camera is JVC TK-C1480BEC using 1/2 inch interlines transfer CCD of 440000(768×576) pixels. The camera lens is COMPUTAR M3Z1228C-MP, which is 2/3 inch industrial camera lens with a zoom range of 12–36

mm and the maximum aperture of 2.8. The CCD camera has been installed on the welding carriage in 20 degrees with the pipeline tangent, and the installation direction is the same as the welding direction. The coordinate plane y-z of CCD camera parallels to the coordinate plane y_0-z_0 of welding wire tip. A narrowband filter of 650±5 nm (transmittance of 10%) and a 9# welding filter have been installed in front of the CCD camera lens. The industrial computer is Advantech IPC-510. The image acquisition card is MeteorII-Standard with 25 fps of sampling rate, and the image acquisition software is VB 6.0. Matlab 7.1 has been used to process the molten pool images.

2.2 Experimental conditions

In the welding experiment of image acquisition for molten pool, the material of the pipeline is Q235 and the groove type is single V groove. The welding method is GMAW with shielding gas of 100% CO_2. The wire is JM-56 (H08Mn2Si) of Jintai. The main parameters of the experiment are shown as Table 1.

Table 1. Main parameters of the experiment

Parameter	Value
Work piece diameter D/mm	325
Work piece thickness δ/mm	10
Wire diameter d/mm	1.2
Groove angle α/(°)	50
Gas-flow rage q/(L • min^{-1})	15–18
Welding current I/A	130–150
Welding speed v_w/(mm • min^{-1})	200–250
Image storage rate v_i/fps	2.8

2.3 Preprocess of the weld pool images

In the process of pipeline butt welding, the original GMAW molten pool images obtained by CCD camera is RGB image of 768×576 pixels as shown in Fig. 2(a), and it must be preprocessed before the operation of extracting the molten pool contour.

(1) First, the molten image is transformed into gray with 8 bit binary number representation 256 gray levels, in which 0 corresponds to black and 255 corresponds to white.

(2) Second, in order to improve the image processing speed, the local image of 180×140 pixels containing the welding molten pool is selected as shown in Fig. 2(b).

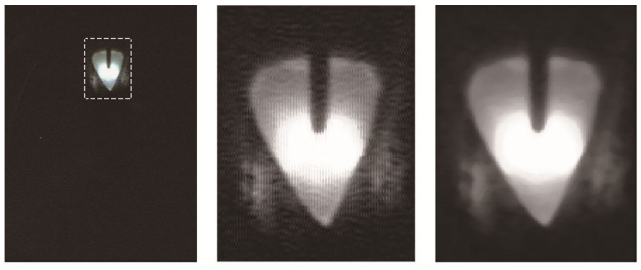

(a) Original image (b) Local image (c) Filtered image

Fig. 2. Preprocess of welding molten pool image

(3) 6×6 templates are selected to do median filtering for the local gray molten pool image. The median filter is a nonlinear smoothing method and is useful to eliminate the interference of spatter and arc light etc in the welding process. The filtered image is shown as Fig. 2(c).

3 Extracting Method of Wavelet Transform for Molten Pool Contour

The welding molten pool images are often disturbed by random noise, and the classical edge detection methods are extremely sensitive to noise because of introducing differential operation in various forms. The wavelet transform has good time-frequency characteristics and is suitable for the singularity of signal detection on account of the multi-resolution analysis of image signal. So it is a powerful tool for image edge processing and will be used for the extraction of welding molten pool image contour.

In the wavelet analysis of multi-resolution, wavelet function $\psi(t)$ and smoothing function $\theta(t)$ are introduced. Let $\theta(t)$ be a two-dimensional smoothing function, and $\iint \theta(x,y)\mathrm{d}x\mathrm{d}y \neq 0$. The derivatives in the two directions of x, y are taken as the two basic wavelets:

$$\psi^{(1)}(x,y)=\frac{\partial\theta(x,y)}{\partial x}, \tag{1}$$

$$\psi^{(2)}(x,y)=\frac{\partial\theta(x,y)}{\partial y}. \tag{2}$$

To make

$$\psi_a^{(1)}(x,y)=\frac{1}{a^2}\psi^{(1)}\left(\frac{x}{a},\frac{y}{a}\right)=\frac{\partial\theta_a(x,y)}{\partial x}, \tag{3}$$

$$\psi_a^{(2)}(x,y)=\frac{1}{a^2}\psi^{(2)}\left(\frac{x}{a},\frac{y}{a}\right)=\frac{\partial\theta_a(x,y)}{\partial y}, \tag{4}$$

where $\theta_a(x,y)=\theta\left(\frac{x}{a},\frac{y}{b}\right)$.

For arbitrary two-dimensional function $f(x,y) \in \boldsymbol{L}^2(\mathbf{R}^2)$, the wavelet transform has two components:

$$\mathbf{WT}^{(i)}f(a,x,y)=f(x,y)*\psi_a^{(i)}(x,y), \tag{5}$$

where signal $*$ represents for the convolution, i=1 or 2. $\mathbf{WT}^{(1)}$ and $\mathbf{WT}^{(2)}$ reflect the image gray gradient along x and y direction. The dyadic wavelet of $f(x,y)$ transform can be abbreviated into vector form:

$$\begin{pmatrix}\mathbf{WT}^{(1)}f(a,x,y)\\ \mathbf{WT}^{(2)}f(a,x,y)\end{pmatrix}=a\times\begin{pmatrix}\frac{\partial}{\partial x}\left(f(x,y)*\theta_a(x,y)\right)\\ \frac{\partial}{\partial y}\left(f(x,y)*\theta_a(x,y)\right)\end{pmatrix}=$$

$$a\times\mathrm{grad}\left(f\left(x,y\right)*\theta_a\left(x,y\right)\right)=a\times\mathrm{grad}\left(f^s\left(x,y\right)\right)=\mathbf{WT}f\left(2^j,x,y\right),\tag{6}$$

where $f^s(x,y)$ is the image smoothed by $\theta_a(x,y)$, $a=2^j$ ($j\in\mathbf{Z}$).

The mode value is

$$\mathrm{Mod}\left(\mathbf{WT}f\left(2^j,x,y\right)\right)=\left(\left|\mathbf{WT}^{(1)}f\left(2^j,x,y\right)\right|^2+\left|\mathbf{WT}^{(2)}f\left(2^j,x,y\right)\right|^2\right)^{\frac{1}{2}}.\tag{7}$$

The argument (angle with the x direction) is

$$\mathrm{Arg}\left(\mathbf{WT}f\left(2^j,x,y\right)\right)=\arctan\left(\frac{\left|\mathbf{WT}^{(2)}f\left(2^j,x,y\right)\right|^2}{\left|\mathbf{WT}^{(1)}f\left(2^j,x,y\right)\right|^2}\right).\tag{8}$$

The image edge is defined as the extremum of Mod(**WT**f), whose direction is Arg(**WT**f) with x direction.

Wavelet transform has the characteristics of energy concentration and can concentrate the signal energy in a few wavelet coefficients. When the image is done wavelet transform by the derivative of the smoothing function as wavelet function, the points of modulus maximum that the wavelet coefficients are greater than a certain threshold value are the edge points of the corresponding image. This is the edge detection principle of wavelet transform[37].

The process of edge contour extraction for weld molten pool image is as follows.

(1) Do discrete dyadic wavelet transform of Haar wavelet for the weld molten pool image after preprocessed, and the matrix of wavelet coefficient is the same size with the matrix of original image.

(2) Obtain the rows and columns wavelet transform coefficients of $\mathbf{WT}^{(1)}f$ (a, x, y), $\mathbf{WT}^{(2)}f$ (a, x, y), and calculate the corresponding wavelet transform modulus and gradient direction according to the Eq. (7). Calculate out respectively the points of local modulus maximum of rows and columns, the points of non maximum are set to 0.

(3) Calculate out the variable threshold $T=G+\mathrm{N}$ by the mean gray of each line, where G is the mean gray of one line and N is a constant. Compare the local modulus maximum with the given threshold T.

(4) Process the edged molten pool image, remove the outliers and false edge points, and get the final edged molten pool image.

The result of edge contour extraction by wavelet transform is shown as Fig. 3. Fig. 3(a) is the original edge contour image, and Fig. 3(b) is the final edge contour image processed by connected region segmentation and others. The final edge contour image is compared with the original welding molten pool shown in Fig. 3(c). It can be seen that the contour of molten pool has been extracted very well by the method of wavelet transform and the key contours such as welding wire and molten pool front tip are coincident well with the original molten pool image .

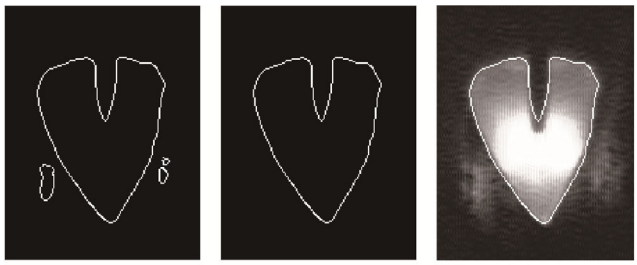

(a) Original contour (b) Processed contour (c) Compared with original contour

Fig. 3. Edge contour extraction of molten pool image

4 Welding Deviation Detection Algorithm

The extracted molten pool contour is a planar curve. The method of contour curvature extremum can be used to search out the position of welding wire and molten pool tip and calculate the welding deviation.

4.1 Physical meaning of contour curvature extremum

For the planar curve C shown in Fig. 4, the curvature of a point P is equal to the reciprocal of osculating circle radius and it is a vector pointing to the circle center. The radius of the osculating circle, which is smaller, is just the radius of curvature that is greater, so the curvature is close to 0 when the curve is close to straight and is large when the curve turning sharply.

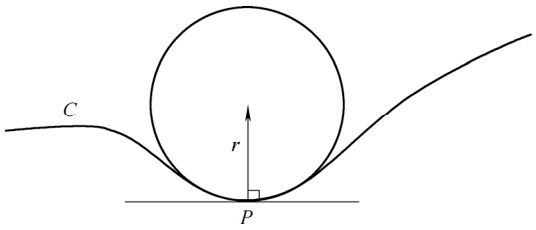

Fig. 4. Principle diagram of planar curve curvature

The molten pool contour (Fig. 3(b)) is shown as Fig. 5 (a) in the x-y coordinate plane of the CCD camera. The contour of welding wire is the most sharply turning part of the whole contour line and is the largest part. The contour of molten pool tip is turning more rapidly than the nearby contour and is the local maximum point.

Selecting a suitable partition line, the molten pool contour can be segmented into two sub contours including welding wire and molten tip separately. For the contour "C" of Fig. 5(a), the partition line greater than y=80 pixel is suitable. Fig. 5(b) shows the two segmented sub contours of "C_1" and "C_2" by the partition line of y=100 pixel. The wire contour is in "C_1" and the molten pool tip contour is in "C_2". So the point of wire center is the maximum curvature point of "C_1" and the point of molten pool tip center is the maximum curvature point of "C_2".

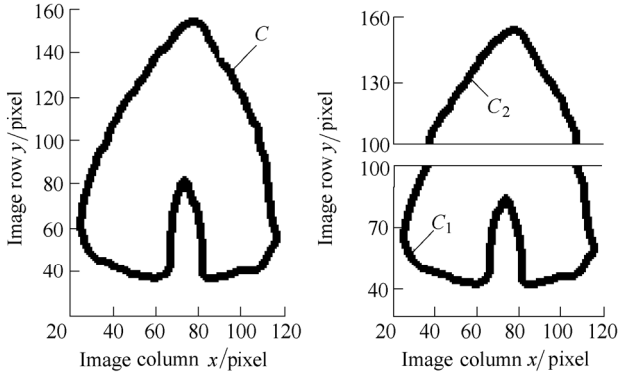

Fig. 5. Molten pool contour and its segmentation map

A test[38] was conducted to compare the images of arcing and arc extinguished as shown in Fig. 6. Fig. 6(a) is the last frame image of the welding molten pool; the pixel coordinate of the molten pool tip center is (310, 294). Fig. 6(b) is the image of arc extinguished; the pixel coordinate of the welded seam groove center is (310, 290). It means that the x axis coordinate value of molten pool tip center coincides with the groove center. Therefore, the molten pool tip center can be used as the same as groove center in the welding deviation algorithm.

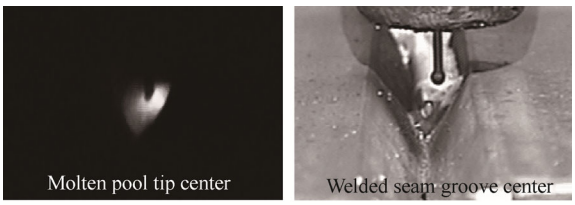

Fig. 6. Image contrast between arcing and arc extinguished

The above analysis shows the physical meaning of contour curvature points for molten pool image that are corresponding to the points of wire center and molten pool center. So the welding deviation can be calculated by the curvature extremum method of contour.

4.2 Curvature extremum algorithm of contour

The curvature of plane curve $y=f(x)$ is

$$k=\frac{\left|f''(x)\right|}{\left[1+f'^2(x)\right]^{3/2}}, \tag{9}$$

and the curvature of plane curve given in a parametric form as $c(t)=(x(t), y(t))$ is

$$k=\frac{\left|x'(t)y''(t)-x''(t)y'(t)\right|}{\left[x'^2(t)+y'^2(t)\right]^{3/2}}. \tag{10}$$

In the x-y coordinates of CCD camera, the molten contour "C" is composed of discrete pixels which can be represented by N of points as $Q_1\cdots Q_i\cdots Q_N$. In the $Q_i=(x_i, y_i)$ of contour "C", considering the three adjacent points and using the difference instead of differential, the contour curvature of the molten pool can be expressed as

$$k_i=\frac{\left|x_i'(t)y_i''(t)-x_i''(t)y_i'(t)\right|}{\left[x_i'^2(t)+y_i'^2(t)\right]^{3/2}}. \tag{11}$$

In Eq. (11),

$$\begin{cases} x_i'=x_{i+1}-x_{i-1}, \\ x_i''=x_{i+1}+x_{i-1}-2x_i, \\ y_i'=y_{i+1}-y_{i-1}, \\ y_i''=y_{i+1}+y_{i-1}-2y_i. \end{cases} \tag{12}$$

This three-points method of curvature formula is simple in calculation but too sensitive to the noise[39]. By selecting m as the step coefficient, the three-point method of Eq. (12) can be expanded into $2m$+1 points method of approximate curvature in practice as Eq. (13). When m is selected reasonable, the approximate curvature of each point can be calculated out and the extremum point can be searched out in the contour of "C_1" and "C_2":

$$\begin{cases} x_i'=x_{i+m}-x_{i-m}, \\ x_i''=x_{i+m}+x_{i-m}-2x_i, \\ y_i'=y_{i+m}-y_{i-m}, \\ y_i''=y_{i+m}+y_{i-m}-2y_i. \end{cases} \tag{13}$$

The curvature of every point is calculated from left to right. There maybe multiple pixels in each column of the extracted contour which are redundant as noise and maybe cause interference on the curvature calculation. Filtering is needed before calculating curvature extremum. In the filtering progress, the contour points of each column are set to be zero but the smallest pixel value point. Fig. 7 shows the resulting of filtering redundant pixels of Fig. 5(b). It can be seen that the filtered sub contour "C_1" missed a part comparing with the original Fig. 5(b).

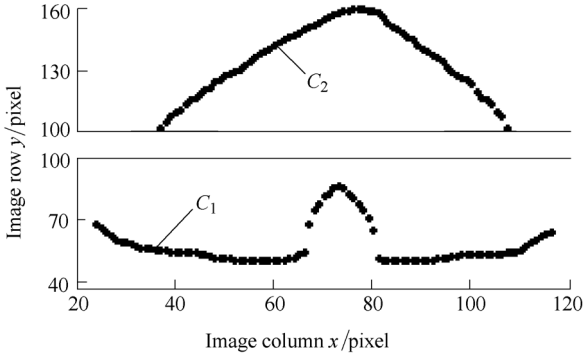

Fig. 7. Filtered contour of molten pool

The program code of searching curvature extremum point for molten pool contour has been written according to

the Eq. (11) and Eq. (13), and the filtered two sub contours of Fig. 7 are calculated separately by setting m=2. Fig. 8 shows the distribution curve of sub contour "C_1" curvature which contains the center information of the wire. Fig. 9 shows the distribution curve of sub contour "C_2" curvature which contains the center information of the molten tip.

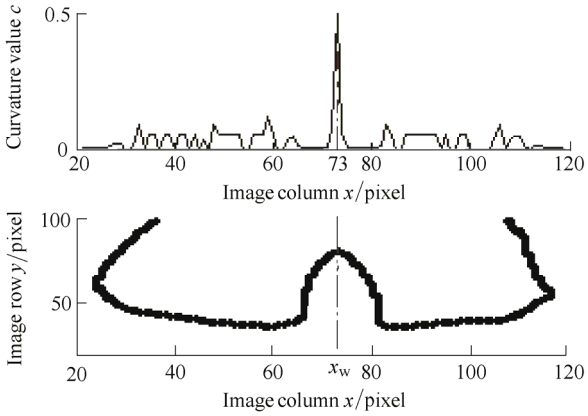

Fig. 8. Distribution curve of sub contour "C_1" curvature

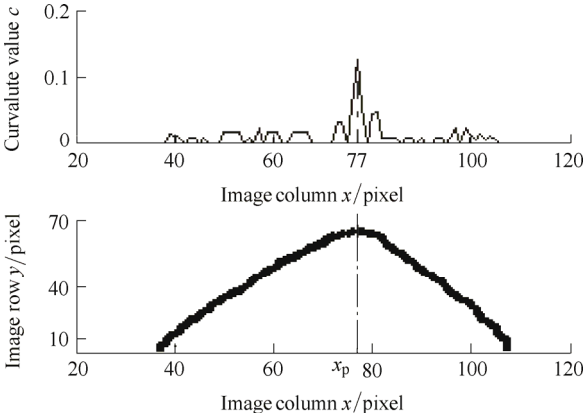

Fig. 9. Distribution curve of sub contour 'C_2' curvature

It can be seen from Fig. 8 and Fig. 9 that the x coordinates of curvature extremum points in the distribution curve of molten pool contour are echoed in the x_w of wire center coordinate and the x_p of molten pool tip center. The pixel value of welding deviation therefore can be calculated by the x coordinate values of extremum points in the two distribution curves.

4.3 Welding deviation calculation

Fig. 10 shows the relationship of the molten pool contour, welding torch, wire, groove and the workpiece.

When the pixel coordinates x_w of wire center and x_p of molten pool tip center are searched out according to the curvature extremum of molten pool contour, the pixel value Δ_p of welding deviation in x direction is

$$\Delta_p = x_w - x_p = \begin{cases} x_w - x_p, & x_w \geqslant x_p, \\ -(x_p - x_w), & x_w < x_p. \end{cases} \tag{14}$$

In Eq. (14), the wire is centre-right when Δ_p is greater than zero, and the wire is centre-left when Δ_p is less than zero.

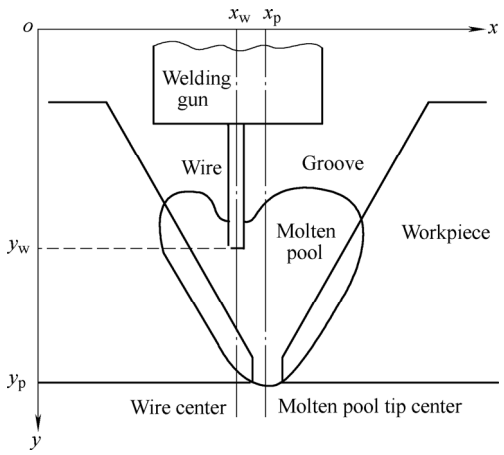

Fig. 10. Principle diagram of weld deviation calculation

The pixel of molten pool image can be calibrated by the wire diameter which is 1.2 mm using in the welding process. In the x-y coordinates, it is about 15 pixels in width between two edges of the wire shown in Fig. 11. So the calibration H of per pixel value is

$$H = \frac{1.2\ \text{mm}}{(81-66)\,\text{Pixel}} = 0.08\ \text{mm} \cdot \text{Pixel}^{-1}. \tag{15}$$

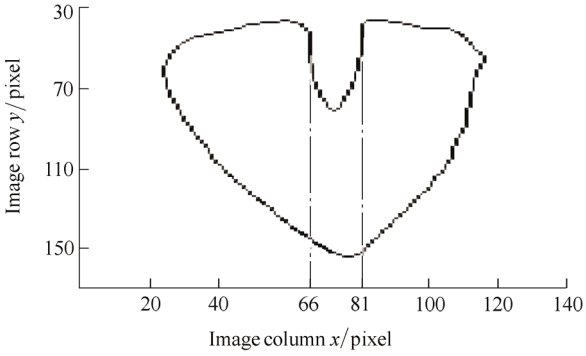

Fig. 11. Schematic diagram of pixel calibration

The real welding deviation Δ_r can be calculated

$$\Delta_r = \Delta_p \times H. \tag{16}$$

The pixel coordinates x_w of wire center is 73 pixels shown in Fig. 7 and the pixel coordinates x_p of molten pool tip center is 77 pixels shown in Fig. 8. The pixel value Δ_p of welding deviation in x direction is calculated out by substituting the two values into Eq. (14):

$$\Delta_p = 73\ \text{Pixel} - 77\ \text{Pixel} = -4\ \text{Pixel}.$$

The real welding deviation Δ_r can be calculated by Eqs. (15) and (16):

$$\Delta_r = \Delta_p \times H = -4\ \text{Pixel} \times 0.08\ \text{mm} \cdot \text{Pixel}^{-1} = -0.32\ \text{mm}.$$

It means that the wire is centre-left for 4 pixels and the

welding deviation is about 0.32 mm.

5 Experimental Analyses

Experiments of pipeline root welding had been done and molten pool images had been obtained in the case of normally no deviation, right deviation, left deviation, and some other than normally circumstances. The welding deviations had been calculated by the proposed curvature extremum algorithm of molten pool contour. And the accuracy, stability and real-time of the proposed algorithm have been analyzed. The experimental condition has been shown in section 1.2.

5.1 Accuracy analysis of the proposed algorithm

To verify the accuracy of the welding deviation algorithm, tests have been designed as follows.

(1) Align the wire with the groove center and start the pipeline downward welding at the circumference position of one o'clock. Deviate the wire gradually from the groove center by artificial intervention and store 100 images continuous with the speed of 2.8 fps in welding process.

(2) By the proposed algorithm, search out the pixel coordinates x_w of wire center and x_p of molten pool tip center, and calculate out the pixel value Δ_p of welding deviation in x direction automatically for each of the 100 stored molten pool images.

(3) Identify manually each of the 100 stored molten pool images and calculate out the x_w, x_p and Δ_p.

(4) Compare the statistical data of x_w, x_p and Δ_p gotten by the proposed algorithm and by the manual, and analyze the accuracy of the proposed algorithm.

Fig. 12 shows the curves of coordinate x_w gotten by the proposed algorithm and by manual. It can be seen that the maximum coordinate deviation between these two curves is 1 pixel. That means the coordinates gotten by the proposed algorithm are well consistent with the manual.

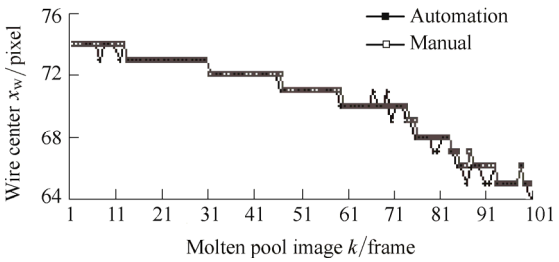

Fig. 12. Comparison curves of wire center x_w

The pixel coordinates x_w of wire center can be used as a constant in theory because the welding gun has been fixed with the CCD camera and the positions of welding wire center should be fixed in the molten pool images. But there are assembly gaps of the welding robot mechanism in reality, and they can make the positions of wire center changed in the welding progress. These are shown in Fig. 12, the pixel coordinates x_w decrease gradually in the welding process and the variation is 9 pixels in the 100 frame images which is about 0.7 mm. So it still needed to detect the pixel coordinates x_w of wire center in the actual progress of welding deviation detection.

Fig. 13 shows the comparison curves of pixel coordinates x_p of molten pool tip center gotten by the proposed algorithm and by manual. The welding wire had been moved fast away from the welding groove center during the experiment as it is shown in Fig. 13: the pixel coordinate x_p changed rapidly nearby the 50th image. The test shown that the coordinates x_p gotten by the proposed algorithm are well consistent with the coordinates x_p gotten by the manual, the maximum coordinates deviation of x_p between these two curves is 1 pixel.

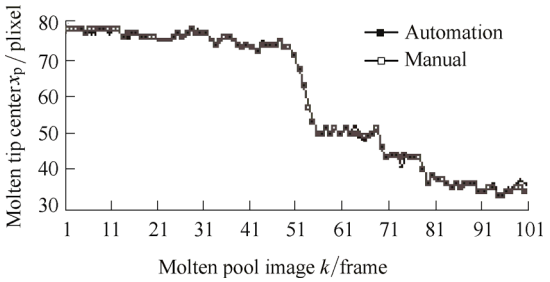

Fig. 13. Comparison curves of molten tip center x_p

Fig. 14 shows the comparison curves of the welding deviation Δ_p gotten by the proposed algorithm and by manual. It can be seen from the Fig. 14 that the maximum welding deviation Δ_p is 2 pixels and the Δ_p gotten by the proposed algorithm are well consistent with the Δ_p gotten by the manual. The welding deviation can be calculated accurately by the proposed algorithm even when the welding deviation is rapidly changed in a short time by the artificial interference.

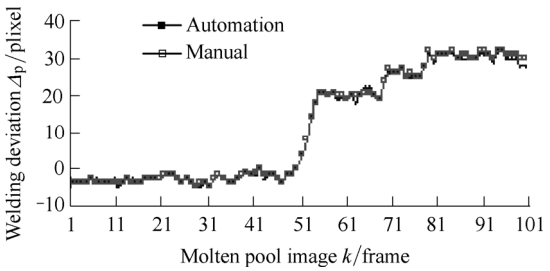

Fig. 14. Comparison curves of welding deviation Δ_p

5.2 Stability analysis of the proposed algorithm

There are many interference factors that affect the welding stability. To verify the stability of the proposed algorithm, the tests have been designed as follows.

(1) Test the stability of the welding deviation algorithm with the interference of arc light and spatter. Change the 9# welding filter to 7# welding filter, while remaining other optical parameters of CCD camera unchanged, and sample and store images of welding molten pool. The acquired images are very bright and there are still other interferences such as smoke, splash, and specular reflection of groove which shows as in Fig. 15(a).

(2) Test the stability of the welding deviation algorithm

to obtain the wire center x_w. Make the wire deviation serious from the center of welding groove and the welding arc burn on the groove edge. It is an irregular shape in the upper part of the molten pool image shown as in Fig. 15(b).

(3) Test the stability of the welding deviation algorithm to extract the molten pool tip center x_p. Move the wire fast from one side of the groove to another side in the process of welding, it makes that there is no obvious tip in the front of the molten pool, as is shown in Fig. 15(c).

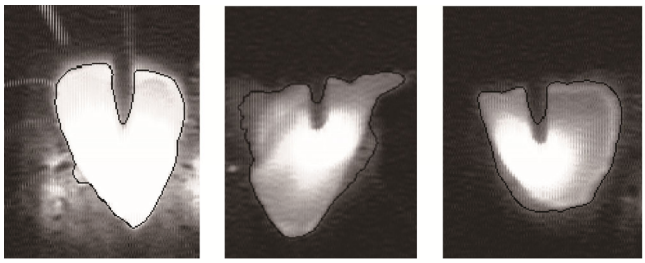

(a) Interference (b) Deviation (c) Inconspicuously tip center

Fig. 15. Images of three kinds of unconventional cases

In the three unconventional cases, the molten pool contours have been extracted by the proposed algorithm showed as the black lines in Fig. 15. The wire center x_w and molten pool tip center x_p of Fig. 15(a), Fig. 15(b) and Fig. 15(c) have been calculated by the proposed algorithm shown as Figs. 16, 17 and 18.

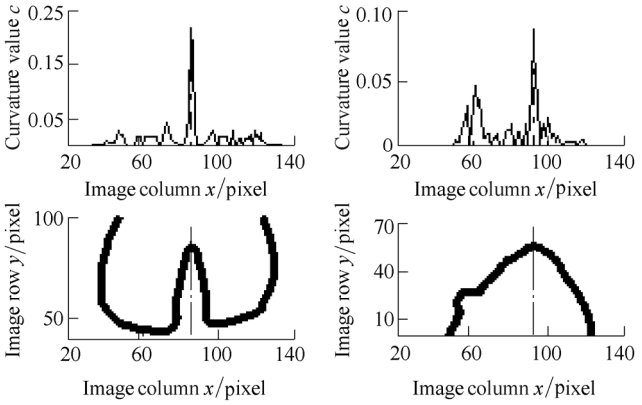

(a) Wire center x_w (b) Molten pool tip center x_p

Fig. 16. Curvature extremum obtained in interference case

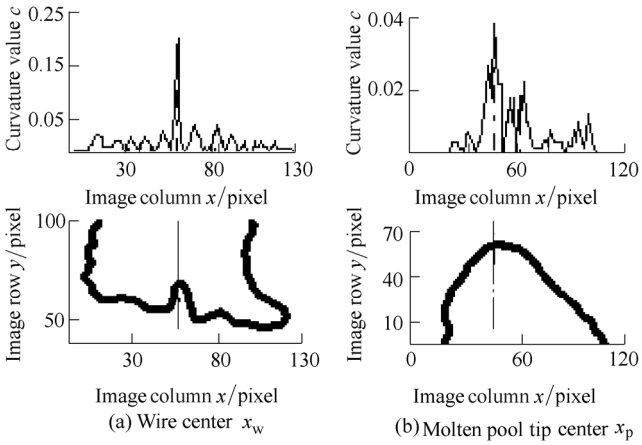

(a) Wire center x_w (b) Molten pool tip center x_p

Fig. 17. Curvature extremum obtained in serious deviation case

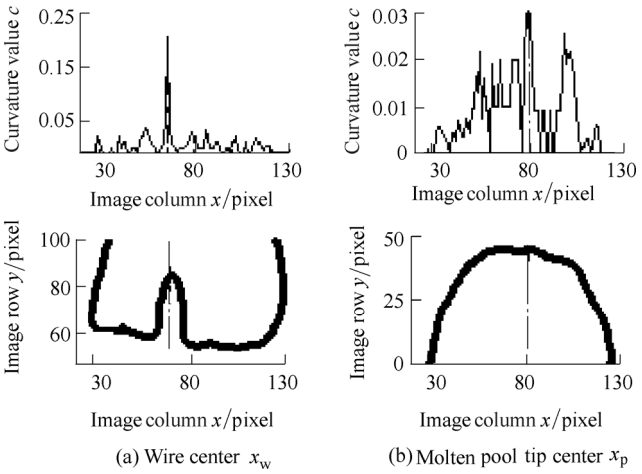

(a) Wire center x_w (b) Molten pool tip center x_p

Fig. 18. Curvature extremum obtained in inconspicuously case

It can be seen that the welding deviation can be obtained exactly by the proposed algorithm in various unconventional cases, which means the algorithm is stable.

5.3 Real-time analysis of the proposed algorithm

The welding deviations were directly calculated by the proposed algorithm in the process of welding. The wire melted in the molten pool, the molten pool tip was in the front direction of the wire. It needs to take some time to move the wire from the pool center to the molten pool tip.

It was about 0.418 061 s for the execution of the proposed welding deviation algorithm program. Take the molten pool contour of Fig. 10 as an example; there were 75 pixels between the wire tip center and the molten pool tip center in y axis which was about 6 mm. When the welding speed was equal to the execution speed of the proposed algorithm program, the speed v_w was the maximum welding speed of real-time control:

$$v_w = \frac{75 \times 0.08}{0.418\,061} \times 60 = 861.12 \text{ mm / min}.$$

The welding speed is less than 500 mm/min in the conventional all-position pipeline welding. Therefore, it is entirely possible to achieve the real-time control of the welding process by the proposed welding deviation algorithm in this paper.

5.4 Other questions to discuss

(1) There are two kinds of welding deviation known as horizontal deviation(x axis) and vertical deviation(y axis), in which horizontal deviation is the more important aspect that affects the welding quality. The length of wire extension is the welding torch height and it has a certain effect on the welding process, but the characteristic of GMAW power is its constant voltage which can self adjust the arc length, and keep the welding process stable when the wire extension changes within a certain range. Therefore, the welding deviation is usually in mean of horizontal deviation in the process of welding tracking. The welding deviation calculated in this paper is especially the

horizontal deviation.

(2) The algorithm of this paper is proposed based on the precondition that the wire center does not coincide with the molten pool tip center. The wire is behind the molten pool tip in the common root welding process. It means that the welding speed is too fast to make the molten pool continuously, but if the wire overlaps with the molten pool tip, the burning through problem will appear which is not allowed in the root welding process. So it is reasonable to divide the molten pool images into two parts for that the wire and molten pool tips should keep separately in the normal root welding process.

6 Conclusions

(1) A kind of the welding deviation detection algorithm is presented via extremum of molten pool image contour.

(2) Welding wire center and molten pool tip center are the key points of the GMAW deviation determination. The physical meaning for the curvature extremum of molten pool contour is that the points of the welding wire center and the molten tip center are the maxima and the local maxima of the contour curvature. Therefore, using the curvature extremum of the molten pool contour to determine the horizontal welding deviation is available.

(3) The welding deviation algorithm includes the contour extracted, the contour line segmented and the contour extremum points obtained. The image contour can be extracted by the proposed method of discrete dyadic wavelet transform, which is divided into two sub contours including welding wire and molten tip separately. The curvature extremum points of the two filtered sub contours can be extracted by using the approximate curvature formula of multi-points plane curve.

(4) The results of the tests and the analyses show that the proposed method can determinate the on-line welding deviation, the maximum error is 2 pixels(0.16 mm), and the algorithm is stable enough to meet the requirements of pipeline real-time control at a speed of less than 500 mm • min^{-1}. This research has provided a new method for on-line automatic welding deviation detection.

References

[1] PRESERN S, GYERGYEK L. An intelligent tactile sensor-an on-line hierarchical object and seam analyzer[J]. *IEEE Transactions on Pattern Analysis and Machine Intelligence*, 1983, PAMI-5(2): 217–219.

[2] SHI Y H, YOO W S, NA S J. Mathematical modeling of rotational arc sensor in GMAW and its applications to seam tracking and endpoint detection[J]. *Science and Technology of Welding and Joining*, 2006, 11(6): 723–730.

[3] HONG Bo, YAN Junguang, YANG Jiawang, et al. A capacitive sensor for automatic weld seam tracking[J]. *Transactions of the China Welding Institution*, 2014, 35(2): 55–58. (in Chinese)

[4] YOU B H, KIM J W. A study on an automatic seam tracking system by using an electromagnetic sensor for sheet metal arc welding of butt joints[J]. *Proceedings of Institution of Mechanical Engineers*, 2002: 911–920.

[5] HU Shengsun, MENG Yingqian, LIU Yong. Development of seam tracking system with ultrasonic sensor using self-tuning fuzzy control[J]. *China Welding*, 2001, 10(1): 39–42.

[6] WU Minsheng, CHEN Wuzhu, HE Fangdian, et al. A seam tracking sensor with modulated infrared beam for arc welding[J]. *Journal of Tsinghua University(Science and Technology)*, 1990, 30(2): 31–36. (in Chinese)

[7] LIU Suyi, WANG Guorong, ZHANG Hua, et al. Design of robot welding seam tracking system with structured light vision[J]. *Chinese Journal of Mechanical Engineering*, 2010, 23(4): 436–442.

[8] JIANG Lipei, XUE Long, ZOU Yong. *Practical technology of welding automation*[M]. Beijing: China Machine Press, 2010. (in Chinese)

[9] ZHANG Y M, KOVACEVIC R, LI L. Characterization and real-time measurement of geometrical appearance of the weld pool[J]. *International Journal of Machine Tools & Manufacture*, 1996, 36(7): 799–816.

[10] XU Yanling, FANG Gu, Lü Na, et al. Computer vision technology for seam tracking in robotic GTAW and GMAW[J]. *Robotics and Computer-Integrated Manufacturing*, 2015, 32: 25–36.

[11] YANG Jiajia, WANG Kehong, WU Tongli, et al. Two-directional synchronous visual sensing and image processing of weld pool in aluminum alloy twin arc pulsed MIG welding[J]. *Journal of Mechanical Engineering*, 2014, 50(12): 44–50. (in Chinese)

[12] ZHANG Guokai, WU Chuansong, LIU Xinfeng. Single vision system for simultaneous observation of keyhole and weld pool in plasma arc welding[J]. *Journal of Materials Processing Technology*, 2015, 215: 71–78.

[13] GAO Jinqiang, QIN Guoliang, YANG Jialin, et al. Image processing of weld pool and keyhole in Nd:YAG laser welding of stainless steel based on visual sensing[J]. *Transactions of Nonferrous Metals Society of China*, 2011, 21(2): 423–428.

[14] BRZAKOVIC D, KHANI D T. Weld pool edge detection for automated control of welding[J]. *IEEE Transactions on Robotics and Automation*, 1991, 7(3): 397–403.

[15] LUO M, SHIN Y C. Vision-based weld pool boundary extraction and width measurement during keyhole fiber laser welding[J]. *Optics and Lasers in Engineering*, 2015, 64: 59–70.

[16] LEONARDO N, RONALD T, FELIX A, et al. Novel algorithm for the real time multi-feature detection in laser beam welding[C]// *IEEE International Symposium on Circuits and Systems(ISCAS)*, COEX, Seoul, Korea, May 20–23, 2012: 181–184.

[17] ZHANG Weijie, LIU Yukang, ZHANG Yuming. Real-time measurement of the weld pool surface in GTAW process[C].//*IEEE International Instrumentation & Measurement Technology Conference*, Minneapolis, USA, May 6–9, 2013: 1640–1645.

[18] XIONG Zhenyu, GU Wangping, WANG Jian, et al. Molten pool image processing and feature extraction based on multiple visions[J]. *Electric Welding Machine*, 2013, 43(5): 93–96. (in Chinese)

[19] ZHANG Gang, SHI Yu, LI Chunkai, et al. Research on the correlation between the status of three-dimensional weld pool surface and weld penetration in TIG welding[J]. *Acta Metallurgica Sinica*, 2014, 50(8): 995–1002. (in Chinese)

[20] JIAO Xiangdong, YANG Yongyong, ZHOU Canfeng. Seam tracking technology for hyperbaric underwater welding[J]. *Chinese Journal of Mechanical Engineering*, 2009, 22(2): 265–269.

[21] HIRAI A, KANEKO Y, HOSODA T, et al. Sensing and control of weld pool by fuzzy-neural network in robotic welding system[C].// *The 27th Annual Conference of the IEEE Industrial Electronics Society*, Denver, USA, November 29–December 02, 2001: 238–242.

[22] GAO Xiangdong, DING Dukun, BAI Tianxiang, et al. Weld pool image centroid algorithm for seam tracking in arc welding process[J]. *IET Image Processing*, 2011, 5(5): 410–419.

[23] FENG Shengqiang, TERASAKI H, KOMIZO Y, et al. Development of evaluation technique of GMAW welding quality based on statistical analysis[J]. *Chinese Journal of Mechanical Engineering*, 2014, 27(6): 1257–1263.

[24] BASKORO A S, ERWANTO, WINARTO. Monitoring of molten pool image during pipe welding in gas metal arc welding(GMAW) using machine vision[C]//*2011 International Conference on Advanced Computer Science and Information System (ICACSIS)*, Jakarta, Indonesia, December 17–18, 2011: 381–384.

[25] LIU J, FAN Z, OLSEN S I, et al, Weld pool visual sensing without external Illumination[C]// *IEEE International Conference on Automation Science and Engineering*, Trieste, Italy, August 24–27, 2011: 145–150.

[26] FAN Fanglei, LI Liangyu, YUE Jianfeng, et al. An image processing arithmetic of the molten pool during GMAW welding[J]. *Mechanical Science and Technology for Aerospace Engineering*, 2008, 27(10): 1199–1201. (in Chinese)

[27] YUE Jianfeng, LI Liangyu, FAN Fanglei, et al. Welding pool adaptive vision detection for arc welding robot gas metal arc welding[J]. *Chinese Journal of Mechanical Engineering*, 2008, 44(4): 206–210. (in Chinese)

[28] LI Jing, QIN Xiaolin, LI Fang, et al. New method based on region coarse localization and Chan-Vese model for weld pool edge extraction in MAG welding[J]. *Journal of Mechanical Engineering*, 2011, 47(12): 74–78. (in Chinese)

[29] WU Mingliang, ZHANG Gang, HUANG Jiankang, et al. Edge detection for aluminum alloy MIG welding pool based on pulse coupled neural network[C]//*Seventh International Conference on Natural Computation*, Shanghai, China, July 26–28, 2011: 691–694.

[30] XUE Jiaxiang, JIA Lin, LI Haibao, et al. Edge detection of molten pool and weld line for CO_2 welding based on B-spline wavelet[J]. *China Welding*, 2004, 13(2): 137–141.

[31] LI Yuan, WANG Qinglin, XU De, et al. Processing and features extraction of molten pool for pipe welding[J]. *Transactions of the China Welding Institution*, 2008, 29(8): 57–60. (in Chinese)

[32] LIU Pengfei, SUN Zhenguo, HUANG Cao, et al. Weld pool image sensor for pulsed MIG welding[J]. *China Welding*, 2008, 17(1):1–5.

[33] LI Jing, LI Fang, ZHU Wei, et al. A new seam location extraction method for pipe-line backing welding of MAG based on passive optical vision sensor[J]. *Transactions of the China Welding Institution*, 2011, 32(10): 69–72. (in Chinese)

[34] BAE K Y, LEE T H, AHN K C. An optical sensing system for seam tracking and weld pool control in gas metal arc welding of steel pipe[J]. *Journal of Materials Processing Technology*, 2002, 120: 458–465.

[35] ZOU Yong, LI Yunhua, JIANG Lipei, et al. Weld pool image processing algorithm for seam tracking of welding robot[C]//*2011 Sixth IEEE Conference on Industrial Electronics and Applications*, Beijing, China, June 21–23, 2011: 155–159.

[36] ZOU Yong, JIANG Lipei, XUE Long, et al. Man-machine interaction system of all-position welding robot of pipeline[J]. *Electric Welding Machine*, 2009, 39(4): 56–58.

[37] TIAN Yanyan, QI Guoqing. Edge detection based on wavelet transform module maxima[J]. *Journal of Dalian Maritime University*, 2007, 33(1): 102–106.

[38] ZOU Yong, LI Yunhua, JIANG Lipei, et al. Method of detecting weld deviation based on molten pool image edge features[J]. *Transactions of the China Welding Institution*, 2015, 36(8): 18–22. (in Chinese)

[39] WANG Yinghui, WU Weiyong, ZHAO Rujia. Segmentation and recognition techniques for planar contour[J]. *Journal of Computer Aided Design & Computer Graphics*, 2002, 14(12): 1142–1145.

Biographical notes

ZOU Yong, born in 1976, is currently a PhD candidate at *Beihang University, China*. He is also a teacher at *Beijing Institute of Petrochemical Technology, China.* He received his master degree from *China University of Petroleum(Beijing), China*, in 2004. His research interests include welding automation and robots.
Tel: +86-10-81292140; E-mail: zouyong@bipt.edu.cn

JIANG Lipei, born in 1942, is currently a professor and a PhD candidate supervisor at *Beijing Institute of Petrochemical Technology, China.* His research interests include welding power and technology, welding automation and underwater welding.
Tel: +86-10-81292220; E-mail: lipei@bipt.edu.cn

LI Yunhua, born in 1963, is currently a professor and a PhD candidate supervisor at *Beihang University, China*. His main research interests include mechachonics, hydraulic control, and robotics.
Tel: +86-10-82339038; E-mail: yhli@buaa.edu.cn

XUE Long, born in 1966, is currently a professor at *Beijing Institute of Petrochemical Technology, China.* His research interests include automation and robotics, underwater welding.
Tel: +86-10-81292242; E-mail: xuelong@bipt.edu.cn

HUANG Junfen, born in 1975, is currently a lecturer at *Beijing Institute of Petrochemical Technology, China*. Her research interests include underwater welding, robotics.
Tel: +86-10-81292140; E-mail: huangjunfen@bipt.edu.cn

HUANG Jiqiang, born in 1971, is currently an associate professor at *Beijing Institute of Petrochemical Technology, China.* His research interests include underwater welding, automation.
Tel: +86-10-81292140; E-mail: huangjiqiang@bipt.edu.cn